Modelling of Thyristor Controlled Series Compensator in Fast Decoupled Load Flow Solution for Power Flow Control

M.Sailaja Kumari, *G.*Priyanka and M. Sydulu

Abstract-- Fast Decoupled Load Flow (FDLF) solution has gained wide spread acceptance in power industry, owing to its simplicity and computational efficiency, but very little attention has been paid for implementation of Thyristor Controlled Series Compensator (TCSC) models in FDLF solutions. This paper addresses the TCSC model implementation in FDLF solution for power flow control. The TCSC firing angle is taken as the state variable, which is combined with nodal voltage angles of the entire network in a unified iterative process while keeping the matrices B′ and B″ constant. The feasibility of the proposed approach is demonstrated and the results of the implementation is tested on IEEE 14 and IEEE 30 bus systems for power flow control in specific branches. The results prove the computational efficiency of FDLF over the NRLF models with TCSC and found to be promising.

Index Terms-- FACTS, Power Flow Control, TCSC, Fast Decoupled Load Flow

I. Introduction

ELECTRIC utilities are operating in an increasingly competitive market where economic and environmental pressures limit their scope to expand transmission facilities. This aspect has provided the momentum for exploring new ways of maximizing the power transfer of existing transmission facilities while at the same time, maintaining the acceptable levels of the network stability and reliability. In this environment high performance control of power network is mandatory. An in depth analysis of options available for achieving such objectives has pointed in the forward direction of FACTS technology [1]. New developments in high current, high-power electronics are making it possible to control electronically the power flows on high voltage side of the network during both steady state and transient operation. One important component is Thyristor Controlled Series Compensator (TCSC), which allows rapid and continuous changes of transmission line impedance [2]. Fig. 1. Shows the TCSC module [2], connected in series with the transmission line. TCSC module consists of a series capacitor bank in parallel with a thyristor controller, shown as bi directional thyristor valve

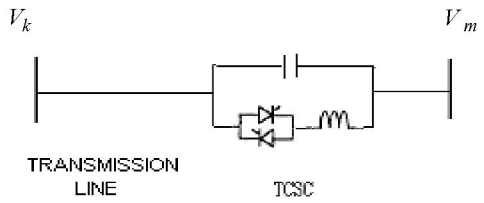

Fig. 1. TCSC module in series with Transmission line

In Load Flow solutions TCSC can be represented in several forms. For instance, the model presented in [3] is based on the concept of variable series compensator whose changing reactance adjusts itself in order to control power flow across the branch to a specified value. The reactance value is determined efficiently by means of Newton's method. The changing reactance represents the fundamental frequency, equivalent reactance of TCSC module. The drawback of this module is that, the firing angle corresponding to the compensation level has to be determined resorting to an iterative process. More over it is not possible to asses within the load flow solution whether or not the solution is taking place in the vicinity of the resonant point. The only indication would be divergent iterative process.

A new TCSC Power Flow model is presented in [4], in which TCSC is adequately represented by its fundamental frequency impedance. The TCSC linearized power flow equations, with respect to the firing angle, are incorporated into an existing Newton-Raphson algorithm. Since the explicit information about the TCSC impedance-firing angle is available [4], good initial conditions are easily selected, hence preventing load flow iterative process from entering the non-operative regions owing to the presence of resonant bands.

The fundamental TCSC equivalent reactance [4] is given by (1)

$$X_{t\,csc} = -X_c + C_1(2(\pi-\alpha)+\sin(2(\pi-\alpha))) - C_2\cos^2(\pi-\alpha)(\varpi\tan(\varpi(\pi-\alpha)) - \tan(\pi-\alpha)) \quad (1)$$

Sailaja Kumari M is with the Department of Electrical Engineering, National Institute of Technology, Warangal, Andhra Pradesh, INDIA.(e-mail: sailaja@nitw.ernet.in)

Priyanka .G is a M.Tech student at the Department of Electrical Engineering, National Institute of Technology, Warangal.

Sydulu .M is also with the Department of Electrical Engineering, National Institute of Technology, Warangal, Andhra Pradesh, INDIA.(e-mail: msydulu@nitw.ernet.in)

1-4244-0273-5/06/$20.00 ©2006 IEEE

Where

$$X_{LC} = \frac{X_C X_L}{X_C - X_L}$$

$$C_1 = \frac{X_C + X_{LC}}{\pi}$$

$$C_2 = \frac{4 X_{LC}^2}{\pi X_L}$$

Fig. 2 shows the TCSC equivalent reactance as a function of firing angle. The behavior of TCSC power flow model is influenced greatly by the number of resonant points in TCSC reactance-firing angle characteristics in the range of 90-180°.

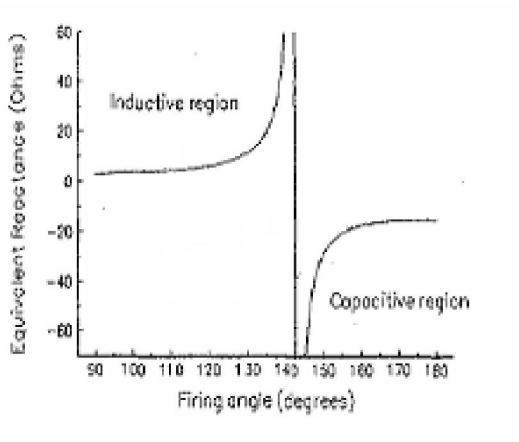

Fig. 2. TCSC equivalent Reactance as a function of firing angle

$$\alpha = \pi(1 - \frac{(2n-1)\omega\sqrt{LC}}{2}) \qquad (2)$$

Where n=1, 2, 3....

Equation (2) is used to determine number of resonant points in the TCSC [2]

As shown in Fig. 2. resonant point exists at α_R=142.81°, for chosen parameters of L and C i.e. X_L=2.6 Ω and X_C=15 Ω [4]. It should be noted that near resonant point, a small variations in the firing angle will induce large changes in both $X_{t\csc}$ and $\partial X_{t\csc}/\partial\alpha$. This in turn may lead to ill conditioned TCSC power equations

II. PROPOSED TCSC POWER FLOW MODELS

Transmission line admittance in which TCSC is placed

$$G_{t\csc} + jB_{t\csc} = \frac{1}{R + j(X + X_{t\csc})}$$

This line admittance is incorporated in bus admittance matrix, and remaining steps are carried out as follows. Power flow equations of the line k-m in which TCSC is placed is given by (3)

$$P_{km}^{\alpha} = V_k^2 G_{t\csc} - V_k V_m (G_{t\csc} Cos(\delta_{km}) + B_{t\csc} Sin(\delta_{km})) \qquad (3)$$

A. Newton Raphson Load Flow (NRLF) Model

When TCSC is used to control power flow in the line k-m, the set of linearised power flow equations are given by (4)

$$\begin{bmatrix} \Delta P_k \\ \Delta P_m \\ \Delta Q_k \\ \Delta Q_m \\ \hline \Delta P_{km}^{\alpha} \end{bmatrix} = \left[\begin{array}{cccc|c} \frac{\partial P_k}{\partial \delta_k} & \frac{\partial P_k}{\partial \delta_m} & \frac{\partial P_k}{\partial V_k}V_k & \frac{\partial P_k}{\partial V_m}V_m & \frac{\partial P_k}{\partial \alpha} \\ \frac{\partial P_m}{\partial \delta_k} & \frac{\partial P_m}{\partial \delta_m} & \frac{\partial P_m}{\partial V_k}V_k & \frac{\partial P_m}{\partial V_m}V_m & \frac{\partial P_m}{\partial \alpha} \\ \frac{\partial Q_k}{\partial \delta_k} & \frac{\partial Q_k}{\partial \delta_m} & \frac{\partial Q_k}{\partial V_k}V_k & \frac{\partial Q_k}{\partial V_m}V_m & \frac{\partial Q_k}{\partial \alpha} \\ \frac{\partial Q_m}{\partial \delta_k} & \frac{\partial Q_m}{\partial \delta_m} & \frac{\partial Q_m}{\partial V_k}V_k & \frac{\partial Q_m}{\partial V_m}V_m & \frac{\partial Q_m}{\partial \alpha} \\ \hline \frac{\partial P_{km}^{\alpha}}{\partial \delta_k} & \frac{\partial P_{km}^{\alpha}}{\partial \delta_m} & \frac{\partial P_{km}^{\alpha}}{\partial V_k}V_k & \frac{\partial P_{km}^{\alpha}}{\partial V_m}V_m & \frac{\partial P_{km}^{\alpha}}{\partial \alpha} \end{array}\right] \begin{bmatrix} \Delta\delta_k \\ \Delta\delta_m \\ \frac{\Delta V_k}{V_k} \\ \frac{\Delta V_m}{V_m} \\ \hline \Delta\alpha \end{bmatrix} \qquad (4)$$

Where, the elements of additional row and column of the modified Jacobean are given by (5)-(13)

$$\frac{\partial P_k}{\partial \alpha} = V_k V_m (-\frac{\partial G_{t\csc}}{\partial \alpha} Cos\ \delta_{km} - \frac{\partial B_{t\csc}}{\partial \alpha} Sin\ \delta_{km}) - V_k^2 \frac{\partial G_{t\csc}}{\partial \alpha} \qquad (5)$$

$$\frac{\partial Q_k}{\partial \alpha} = V_k V_m (\frac{\partial G_{t\csc}}{\partial \alpha} Sin\ \delta_{km} - \frac{\partial B_{t\csc}}{\partial \alpha} Cos\ \delta_{km}) - V_k^2 \frac{\partial B_{t\csc}}{\partial \alpha} \qquad (6)$$

$\frac{\partial P_m}{\partial \alpha}, \frac{\partial Q_m}{\partial \alpha}$ Can be obtained by replacing k by m and vice versa in the above equations. In (5) and (6)

$$\frac{\partial G_{t\csc}}{\partial \alpha} = \frac{-2R(X + X_{t\csc})}{(R^2 + (X + X_{t\csc})^2)^2} \frac{\partial X_{t\csc}}{\partial \alpha} \qquad (7)$$

$$\frac{\partial B_{t\csc}}{\partial \alpha} = -\frac{1}{R^2 + (X + X_{t\csc})^2)^2} (\frac{\partial X_{t\csc}}{\partial \alpha}) + \frac{2(X + X_{t\csc})^2}{(R^2 + (X + X_{t\csc})^2)^2} (\frac{\partial X_{t\csc}}{\partial \alpha}) \qquad (8)$$

In (7) and (8)

$$\frac{\partial X_{t\csc}}{\partial \alpha} = -2C_1 (1 + Cos 2\alpha) + C_2 Sin(2\alpha)(\varpi \tan(\varpi(\pi - \alpha)) + \tan\alpha) + C_2 (\varpi^2 \frac{Cos^2(\pi - \alpha)}{Cos^2(\varpi(\pi - \alpha))} - 1) \qquad (9)$$

Also the elements of the added row in (4)

$$\frac{\partial P_{km}^{\alpha}}{\partial \alpha} = V_k^2 \frac{\partial G_{t\csc}}{\partial \alpha} - V_k V_m (\frac{\partial G_{t\csc}}{\partial \alpha} Cos(\delta_{km}) + \frac{\partial B_{t\csc}}{\partial \alpha} Sin(\delta_{km})) \qquad (10)$$

$$\frac{\partial P_{km}}{\partial \delta_k} = -V_k V_m (-G_{t\csc} Sin\ \delta_{km} + B_{t\csc} Cos\ \delta_{km}) \qquad (11)$$

$$\frac{\partial P_{km}^{\alpha}}{\partial \delta_m} = -\frac{\partial P_{km}^{\alpha}}{\partial \delta_k} \qquad (12)$$

$$\frac{\partial P_{km}^{\alpha}}{\partial V_k} V_k = P_{km}^{\alpha} + Vk_k^2 G_{t\csc} \qquad (13)$$

$$\frac{\partial P_{km}^{\alpha}}{\partial V_m} V_m = P_{km}^{\alpha} - V_k^2 G_{t\csc} \qquad (14)$$

In the mismatch vector of (4)

$\Delta P_{km}^{\alpha} = P_{km}^{req} - P_{km}^{\alpha}$ is the active power flow mismatch for the TCSC module. P_{km}^{req} is the required power flow in the TCSC branch.

Now solve for system variables along with the firing angle mismatch using (4), making use of modified Jacobean matrix

Update the firing angles using the following equation

$\alpha^{i+1} = \alpha^{i} + \Delta\alpha$, Where $\Delta\alpha$ is the incremental change in the TCSC's firing angle and i shows i^{th} iteration

B. Fast Decoupled Load Flow (FDLF) model

FDLF is based on the assumption that during normal operation incremental changes in voltage magnitudes produce almost no change in active power and incremental changes in voltage angles produces no change in reactive power flow. Hence steady state operation is assessed by iterative solution of the following set of equations

$$\left[\frac{\Delta P}{V}\right] = [B'][\Delta\delta]$$
$$\left[\frac{\Delta Q}{V}\right] = [B''][\Delta V]$$

Where ΔP and ΔQ are active and reactive power mismatches, Δδ and ΔV are vectors of incremental changes in nodal voltage angles and magnitudes, while B' and B'' are the constant slope matrices of the standard FDLF BX (Amerongen) model, whose elements are

$$B'_{pq} = -B_{pq}$$
$$B'_{pp} = -B_{pp}$$
$$B''_{pq} = -X_{pq}^{-1}$$
$$B''_{pp} = \sum_{q\in p} X_{pq}^{-1}$$

$q \in p$ is set of nodes adjacent to node p. When TCSC is used for active power flow control of the line k-m, the modified FDLF power flow equations are given by (15) and (16)

$$\begin{bmatrix} \frac{\Delta P_k}{V} \\ \frac{\Delta P_m}{V} \\ \hline \Delta P^{\alpha}_{km} \end{bmatrix} = \left[\begin{array}{ccc} & B' & \\ & & \\ \hline \frac{\partial P^{\alpha}_{km}}{\partial\delta_k} & \frac{\partial P^{\alpha}_{km}}{\partial\delta_m} & \frac{\partial P^{\alpha}_{km}}{\partial\alpha} \end{array}\right] \begin{bmatrix} \frac{\partial P_k}{\partial\alpha} \\ \frac{\partial P_m}{\partial\alpha} \\ \hline \Delta\alpha \end{bmatrix} \begin{bmatrix} \Delta\delta_k \\ \Delta\delta_m \\ \hline \Delta\alpha \end{bmatrix} \quad (15)$$

$$\left[\frac{\Delta Q}{V}\right] = [B''][\Delta V] \quad (16)$$

Where for the TCSC branch k-m

$$B'_{km} = -B_{km}$$
$$B'_{kk} = -B_{kk}$$
$$B''_{kk} = \sum_{m\in k} (X_{km} + X_{t\,\mathrm{csc}})^{-1}$$
$$B''_{km} = -(X_{km} + X_{t\,\mathrm{csc}})^{-1}$$

$m \in k$ is set of nodes adjacent to node k. B_{km} and B_{kk} are imaginary part of corresponding admittances of nodal admittance matrix including changes due to TCSC.

The elements of added row and column of modified slope matrix in (15) are given by (17)-(19)

$$\frac{\partial P_k}{\partial\alpha} = V_k V_m\left(-\frac{\partial G_{t\,\mathrm{csc}}}{\partial\alpha}Cos\delta_{km} - \frac{\partial B_{t\,\mathrm{csc}}}{\partial\alpha}Sin\delta_{km}\right) - V_k^2\frac{\partial G_{t\,\mathrm{csc}}}{\partial\alpha} \quad (17)$$

$\frac{\partial P_m}{\partial\alpha}$ Can be obtained by replacing k by m and vice versa in the above equation

$$\frac{\partial P^{\alpha}_{km}}{\partial\alpha} = V_k^2\frac{\partial G_{t\,\mathrm{csc}}}{\partial\alpha} - V_k V_m\left(\frac{\partial G_{t\,\mathrm{csc}}}{\partial\alpha}Cos\delta_{km} + \frac{\partial B_{t\,\mathrm{csc}}}{\partial\alpha}Sin\delta_{km}\right) \quad (18)$$

$$\frac{\partial P^{\alpha}_{km}}{\partial\delta_k} = -V_k V_m\left(-G_{t\,\mathrm{csc}}Sin\,\delta_{km} + B_{t\,\mathrm{csc}}Cos\,\delta_{km}\right) \quad (19)$$

$$\frac{\partial P^{\alpha}_{km}}{\partial\delta_m} = -\frac{\partial P^{\alpha}_{km}}{\partial\delta_k} \quad (20)$$

In (17) and (18)

$$\frac{\partial G_{t\,\mathrm{csc}}}{\partial\alpha} = \frac{-2R(X+X_{t\,\mathrm{csc}})}{(R^2+(X+X_{t\,\mathrm{csc}})^2)^2}\frac{\partial X_{t\,\mathrm{csc}}}{\partial\alpha} \quad (21)$$

$$\frac{\partial B_{t\,\mathrm{csc}}}{\partial\alpha} = -\frac{1}{R^2+(X+X_{t\,\mathrm{csc}})^2)^2}\left(\frac{\partial X_{t\,\mathrm{csc}}}{\partial\alpha}\right) + \frac{2(X+X_{t\,\mathrm{csc}})^2}{(R^2+(X+X_{t\,\mathrm{csc}})^2)^2}\left(\frac{\partial X_{t\,\mathrm{csc}}}{\partial\alpha}\right) \quad (22)$$

In (21) and (22)

$$\frac{\partial X_{t\,\mathrm{csc}}}{\partial\alpha} = -2C_1(1+Cos\,2\alpha) + C_2 Sin(2\alpha)(\varpi Tan(\varpi(\pi-\alpha)) + \tan\alpha) + C_2\left(\varpi^2\frac{\cos^2(\pi-\alpha)}{\cos^2(\varpi(\pi-\alpha))} - 1\right) \quad (23)$$

$\Delta P_{km} = P^{req}_{km} - P^{\alpha}_{km}$ is the active power flow mismatch for the TCSC module

Ill chosen initial conditions are often responsible for load flow solution diverging or arriving at some anomalous value. In order to avoid this, small difference in voltage angles at TCSC buses is also considered, in this FDLF model for extra row and column in (15) the following assumption is not considered

$$\cos\,\delta_{km} \cong 1$$
$$\sin\,\delta_{km} \cong 0$$

The initial condition for the TCSC's firing angle is selected within the range of $\pm 8^0$ from the resonant point [4]. Update the firing angles using the following equation $\alpha^{i+1} = \alpha^{i} + \Delta\alpha$, where $\Delta\alpha$ is the incremental change in the TCSC's firing angle in i^{th} iteration. 1δ 1V scheme is used for iterative solution

III. CASE STUDIES

In order to demonstrate the performance of the FDLF with TCSC device for power flow control, IEEE 14 and IEEE 30 bus systems are considered. To obtain power flow solutions with TCSC Xc =2.6Ω and X_l =15Ω [2] are considered. The range of reactance of the installed TCSCs is appropriately chosen between -70% to +20% of existing line reactance (i.e-0.7*X to* 0.2X*)* where *X* is the reactance of the corresponding transmission line in which installation of TCSCs are desired.

TABLE I
NEWTON-RAPHSON LOAD FLOW RESULTS FOR IEEE 14-BUS SYSTEM WITH TCSC

Line No. in which TCSC is placed	2	4	5
Alpha Final (degree)	162.661	30.321	166.7471
Xtcsc (pu)	-0.0407	+0.0295	-0.0510
Compensation (%)	-20.593	+13.269	-29.330
Power flow with out TCSC (MW)	73.342	75.440	41.521
Specified power flow with TCSC (MW)	80.00	70.00	50.00

Table I shows the results of TCSC implementation in NRLF for power flow control. The real power flows in the line number 2, 4 and 5 without TCSC devices are 73.342, 75.44 and 41.521MW, respectively. An attempt is now been made to control the real power flows in the above-mentioned lines to a specified power flow of 80, 70, and 50MW, respectively using TCSC devices. The value of X_{tcsc} both in PU, as % of line reactance and its corresponding firing angle (α_{final}) to meet the above mentioned desired power flow are tabulated.

TABLE II
FAST DECOUPLED LOAD FLOW RESULTS FOR IEEE 14-BUS SYSTEM WITH TCSC

Line No. in which TCSC is placed	2	4	5
Alpha Final (degree)	162.566	30.298	166.752
Xtcsc (pu)	-0.0405	+0.0296	-0.0510
Compensation (%)	-20.480	+13.28	-29.340
Power flow with out TCSC (MW)	73.342	75.440	41.521
Specified power flow with TCSC (MW)	80.00	70.00	50.00

Table II shows the results of TCSC implementation in FDLF for power flow control in the selected lines 2, 4 and 5, which are almost similar to the results obtained using NRLF.

Similarly the effectiveness of the model is tested on IEEE 30 bus system and the results are presented in the Table III and Table IV.

TABLE III
NEWTON-RAPHSON LOAD FLOW RESULTS IEEE 30-BUS SYSTEM WITH TCSC

Line No.in which TCSC is placed	2	3	15
Alpha Final (degree)	166.185	14.09	170.990
Xtcsc (pu)	-0.0495	+0.055	-0.0620
Compensation (%)	-26.770%	+31.77%	-24.240%
Power flow with out TCSC (MW)	48.221	29.290	27.293
Specified power flow with TCSC (MW)	55.00	25.00	30.00

TABLE IV
FAST DECOUPLED LOAD FLOW RESULTS FOR IEEE 30-BUS SYSTEM WITH TCSC

Line No. in which TCSC is placed	2	3	15
Alpha Final (degree)	166.170	14.0566	170.893
Xtcsc (pu)	-0.0495	+0.0551	-0.0618
Compensation (%)	-26.750	+31.73	-24.140
Power flow with out TCSC (MW)	48.221	29.290	27.293
Specified power flow with TCSC (MW)	55.00	25.00	30.00

A comparison is now made between NRLF and FDLF solutions considering the time of convergence. Tables V and VI show the number of iterations and the time taken for convergence in both the cases.

Tables V and VI demonstrate the superior convergence of FDLF with TCSC over NRLF models. Even though the number of iterations to converge is more with FDLF model, the time of convergence is very small , because of the fact that the time per iteration is considerably reduced with FDLF.

TABLE V
COMPARISON OF NUMBER OF ITERATIONS AND TIME OF CONVERGENCE FOR IEEE 14 BUS SYSTEM

	Base case		TCSC in line no.2		TCSC in line no.4	
	NRLF	FDLF	NRLF	FDLF	NRLF	FDLF
Number of Iterations to converge	3	4	9	12	17	18
Time of convergence in sec	0.12	0.04	0.31	0.192	0.588	0.288

TABLE V1
COMPARISON OF NUMBER OF ITERATIONS AND TIME OF CONVERGENCE FOR IEEE 30 BUS SYSTEM

	Base case		TCSC in line no.2		TCSC in line no.4	
	NRLF	FDLF	NRLF	FDLF	NRLF	FDLF
Number of Iterations to converge	3	3.5	10	14	9	10
Time of convergence in sec	0.125	0.056	0.36	0.22	0.27	0.15

Now variation of active power flow mismatches with time of convergence is plotted for both NRLF and FDLF power flows with TCSC device.

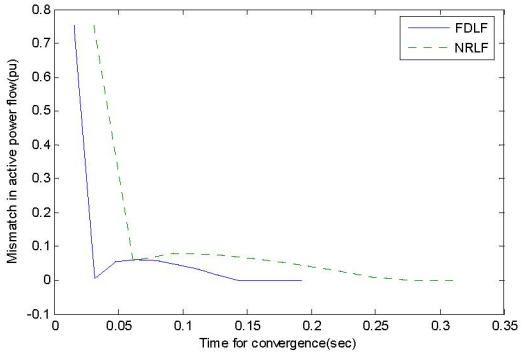

Fig. 3. Tcsc placed in line 2 of IEEE14 bus system with scheduled power flow of 80MW

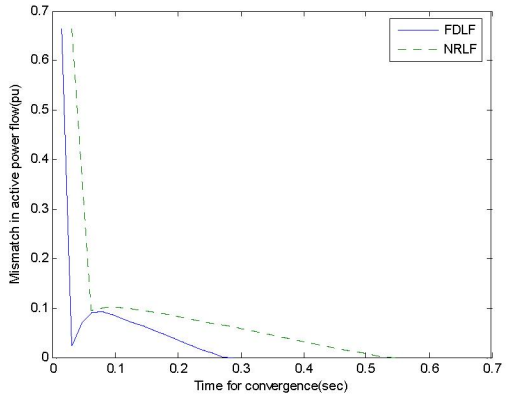

Fig. 4. Tcsc placed in line 4 of IEEE14 bus system with scheduled active power flow of 70MW

Figs. 3 and 4 show the convergence characteristics when TCSC is placed in line no.s 2 and 4 of IEEE14 bus system to enhance the power flow in line 2 to 80MW and limit the power flow in line4 to 70MW respectively.

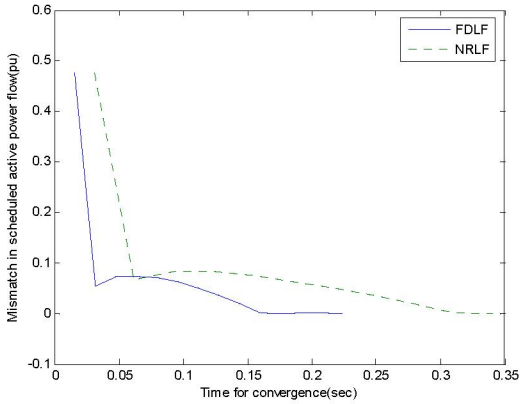

Fig. 5. Tcsc placed in line 2 of IEEE 30 bus system with scheduled active power flow of 55.MW

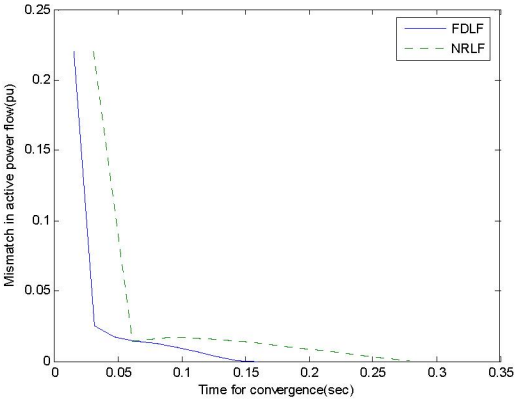

Fig. 6. Tcsc placed in line 3 of IEEE 30 bus system with scheduled active power flow of 25 MW

Fig. 5 and 6 show the convergence characteristic of power flow mismatch in line no. 2 and 3 of IEEE 30bus system to enhance the power flow in line 2 to 55MW and to limit the power flow in line 3 to 25MW. From the graphs it is obvious that the FDLF model shows faster convergence even with incorporation of TCSC

IV. CONCLUSIONS

In this paper a Fast Decoupled Load Flow incorporating TCSC firing angle model has been developed. The model takes care of the starting voltage angles at the TCSC buses, which if neglected will lead to divergence of the algorithm. The FDLF model shows faster convergence compared to NRLF model due to its computational efficiency. The results obtained using FDLF and NRLF incorporating TCSC model for IEEE 14 and 30 bus systems are compared and found to be same.

V. REFERENCES

[1] N. H. Hingorani, "Flexible AC transmission systems" , IEEE Spectrum, p.p 4045, Apr. 1993

[2] N. Cbristl, R. Hcdin, k Sadck, P. Llitzelberger,P.E. Krduse, S.M. McKcnna, A. H. Maiitaya, and D. Togerson, "Advanced series compensiuion (ASC) with thyristor controllcd impedance," in ***Int. Conf Large High Voltage Electric Sysrems*** *(CIGRE),* Paris, Sept. 1992, Paper 14/37/38-05.

[3] Scott G. Helbing, G.G. Karaday, "Investigations on an advanced form of Series Compensation", IEEE Transactions on Power Delivery, Vol. 9, No 2, April 1994. 14/37/38-07.

[4] R. Fuerte-Esquivel, E. Acha, and H. Ambriz-Pbrez, "A Thyristor Controlled Series Compensator Model for the Power Flow Solution of Practical Power Networks", IEEE transactions on power systems vol 15 no.1, Feb 2000.

[5] B. Stott and O. Alsac, "Fast decoupled load flow," *IEEE Trans. Power App. Syst.*, vol. PAS-93, no. 2, pp. 859–869, May 1974.

[6] J.H.Tovar-Hernandez, C.R. Fuerte-Esquivel, member ,IEEE and V.M. Chavez- Ornelas, "Modeling of Static VAR's Compensator in Fast Decoupled Load Flow", IEEE Transactions on power systems, vol.20, no.1, February 2005.

[7] Narayana Prasad Padhy., M.A. Abdel Moamen, "Power flow control and solutions with multiple and multi-type FACTS devices", Electric Power Systems Research 74 (2005) pp.341–351